The ATP-P2X$_7$ Signaling Axis Is Dispensable for Obesity-Associated Inflammasome Activation in Adipose Tissue

Shengyi Sun,[1] Sheng Xia,[2] Yewei Ji,[2] Sander Kersten,[2,3] and Ling Qi[1,2]

Inflammasome activation in adipose tissue has been implicated in obesity-associated insulin resistance and type 2 diabetes. However, when and how inflammasome is activated in adipose tissue remains speculative. Here we test the hypothesis that extracellular ATP, a potent stimulus of inflammasome in macrophages via purinergic receptor P2X, ligand-gated ion channel, 7 (P2X$_7$), may play a role in inflammasome activation in adipose tissue in obesity. Our data show that inflammasome is activated in adipose tissue upon 8-week feeding of 60% high-fat diet (HFD), coinciding with the onset of hyperglycemia and hyperinsulinemia as well as the induction of P2X$_7$ in adipose tissue. Unexpectedly, *P2X$_7$*-deficient animals on HFD exhibit no changes in metabolic phenotypes, inflammatory responses, or inflammasome activation when compared with the wild-type controls. Similar observations have been obtained in hematopoietic cell–specific *P2X$_7$*-deficient animals generated by bone marrow transplantation. Thus, we conclude that inflammasome activation in adipose tissue in obesity coincides with the onset of hyperglycemia and hyperinsulinemia but, unexpectedly, is not mediated by the ATP-P2X$_7$ signaling axis. The nature of the inflammasome-activating danger signal(s) in adipose tissue in obesity remains to be characterized. ***Diabetes*** **61:1471–1478, 2012**

Obesity is a major health threat in both developing and developed countries and poses a significant risk factor for type II diabetes, arthritis, cardiovascular diseases, and even cancer. The progression of obesity is strongly associated with chronic inflammation in white adipose tissue (WAT) (1–4). Genetic studies in mice and clinical studies in humans have shown that downregulation of the inflammatory response in WAT is associated with improvement of systemic glucose homeostasis and insulin sensitivity (5).

Proinflammatory cytokines such as interleukin-1β and -18 (IL-1β and -18) secreted by adipose tissue have been linked to insulin resistance during obesity (6–9). The maturation of IL-1β and IL-18 requires the activation of inflammasomes, including NLRP1 (Nod-like receptor family, pyrin domain containing 1), NLRP3, NLRC4 (Nod-like receptor family, caspase activation and recruitment domain containing 4), and AIM2 (absent in melanoma 2) inflammasome (10). The most well-studied inflammasome is NLRP3 inflammasome, a multiprotein complex consisting of NLRP3, ASC (apoptosis-associated speck-like protein containing COOH-terminal caspase activation and recruitment domain), and a cysteine protease caspase-1. The activation of inflammasome induces the cleavage of procaspase-1 to active caspase-1, which in turn processes pro–IL-1β and pro–IL-18 to bioactive IL-1β and IL-18 to be released (11). Several recent studies have demonstrated that the NLRP3 inflammasome is important for obesity-associated inflammation and the development of insulin resistance (12–15). Indeed, mice deficient in caspase-1 or NLRP3 were protected against obesity-associated inflammation and insulin resistance with reduced circulating IL-18, reduced IL-1β and effector T cells in adipose tissue, and improved systemic insulin sensitivity (12–15). However, it remains unclear when and how inflammasome is activated in high-fat diet (HFD) feeding.

Studies on the immune system have revealed that the activation of inflammasome, or synthesis, processing, and release of mature IL-1β by macrophages, ex vivo requires two stimuli: first, an inflammatory stimulus, such as lipopolysaccharide (LPS), primes cells to transcribe and synthesize pro–IL-1β, and then a second stimulus, such as ATP, nigericin, or bacterial toxins, is required for optimal inflammasome activation and maximal IL-1β release (10). An outstanding question with regards to inflammasome activation in obesity is what the two activating stimuli are in adipose tissue. Stimuli including ATP, glucose, or lipids such as palmitate and ceramides have been suggested to play a role in inflammasome activation in obese adipose tissue (12,14–16). However, physiological relevance and importance of these stimuli have not been documented with in vivo studies.

Extracellular ATP is a potent inflammasome-activating signal both in vitro and in vivo in some disease settings such as cancer, graft-versus-host disease, hypersensitivity, and sterile inflammation (17–21). Among the several purinergic receptors capable of ATP sensing (P2X$_{1–7}$ and P2Y$_{1–2, 4, 11, 12}$), P2X$_7$ (also known as P2RX$_7$) is unique in its ability to activate inflammasome (22). P2X$_7$ is a cell-surface ion channel receptor activated by a high level of extracellular ATP and subsequently allows rapid efflux of potassium ions to activate inflammasome (17,23–25). In vivo, extracellular ATP can be released from apoptotic and necrotic cells as a "danger signal" to upregulate inflammation in a P2X$_7$-dependent manner (18–21,26), suggesting an interesting mechanism by which dying cells regulate inflammasome activation. Intriguingly, obesity is associated with increased cell death in adipose tissue and the aggregation of macrophages around dead cells, also known as "crown-like structure" (27–30). It has been suggested that adipocyte cell death may contribute to the progression of inflammation in adipose tissue (29,31), although this remains

From the [1]Graduate Program in Biochemistry, Molecular, and Cell Biology, Cornell University, Ithaca, New York; the [2]Division of Nutritional Sciences, Cornell University, Ithaca, New York; and the [3]Nutrition, Metabolism, and Genomics Group, Division of Human Nutrition, Wageningen University, Wageningen, the Netherlands.
Corresponding author: Ling Qi, lq35@cornell.edu.
Received 3 October 2011 and accepted 7 February 2012.
DOI: 10.2337/db11-1389
This article contains Supplementary Data online at http://diabetes.diabetesjournals.org/lookup/suppl/doi:10.2337/db11-1389/-/DC1.
S.X. is currently affiliated with the Department of Immunology, Jiangsu University School of Medicine, Jiangsu, China.

controversial (30). How cell death is linked to inflammation or inflammasome activation in obesity remains a mystery.

Here we addressed whether extracellular ATP links obesity, obesity-associated cell death, and inflammasome activation in adipose tissue via its receptor P2X$_7$. Our data show that induction of both P2X$_7$ expression and inflammasome activation in adipose tissue started at 8-week feeding of 60% HFD, coinciding with the onset of hyperglycemia and hyperinsulinemia. However, to our surprise, the ATP-P2X$_7$ signaling axis is dispensable for inflammasome activation in obese adipose tissue.

RESEARCH DESIGN AND METHODS

Mouse models. Wild-type (WT) C57/B6 (*CD45.2*$^+$; 000664), B6.129P2-*P2rx7*^{tm1Gab}/J (*P2X*$_7^{-/-}$; 005576), B6.129P2-*P2ry2*^{tm1Bhk}/J (*P2Y*$_2^{-/-}$; 009132), B6.SJL-*Ptprc*^{a} *Pepc*^{b}/BoyJ (*CD45.1*$^+$; 002014), and B6.V-*Lep*^{ob}/J (*ob/ob*; 000632) mice were purchased from The Jackson Laboratory and bred in our facility. The *P2X*$_7^{-/-}$ and *P2Y*$_2^{-/-}$ mice had been back-crossed to the B6 background for 7 and 12 generations, respectively. WAT tissue lysates from 16-week HFD *caspase-1*$^{-/-}$ mice were provided by Dr. Rinke Stienstra (Wageningen University). Mice were housed in our pathogen-free facility with 13% low-fat diet (LFD), with 13% fat, 67% carbohydrate, and 20% protein from Harlan Teklad (2914), and at 6 weeks of age were placed on 60% HFD, with 60% fat, 20% carbohydrate, and 20% protein from Research Diets Inc. (D12492). All animal procedures were approved by the Cornell Institutional Animal Care and Use Committee.

Metabolic phenotyping. Six-week-old male mice were fed with either 13% LFD or 60% HFD for the indicated period of time from 1 to 29 weeks. For GTT, mice were fasted for 16–18 h followed by an injection of glucose (Sigma) at 1 g/kg body weight (BW). For ITT, mice were fasted for 5 h followed by an injection of insulin (Sigma) at 36 μg/kg BW. Blood glucose was monitored using One-Touch Ultra (LifeScan) or AlphaTRAK Glucometer (Abbott). Fasting insulin levels were measured after a 4-h fast. Mice were killed by cervical dislocation, and tissues were either fixed for histology or snap frozen in liquid nitrogen for quantitative PCR (Q-PCR) and Western blot analyses. Frozen tissues were stored at −80°C.

LPS/ATP challenge in vivo. Eight-week-old WT or *P2X*$_7^{-/-}$ mice were injected intraperitoneally with LPS at 2 ng/g BW (L4130; Sigma) 1.5 h prior to the ATP challenge intraperitoneally (50 mM ATP, adjusted to pH 7 with NaOH; Sigma) at 10 μL/g BW. One hour later, mice were killed and blood serum was collected.

Bone marrow transplantation. Bone marrow was obtained by flushing the femurs from sex-matched donor mice with PBS. Eight-week-old recipient male mice were lethally irradiated (10 Gy) and transplanted with 5 million bone marrow cells via intravenous injection. One week prior to and 2 weeks after bone marrow transplantation (BMT), 2 mg/mL neomycin (Cellgro) was added to drinking water. After 4 weeks recovery, recipients were placed on 60% HFD for 16 weeks prior to metabolic phenotyping.

Isolation of primary adipocytes and stromal vascular cells. Epididymal fat pads were collected and minced with razor blades. After two washes with KRBH buffer (10 mmol/L HEPES, pH 7.4, 15 mmol/L $NaHCO_3$, 120 mmol/L NaCl, 4 mmol/L KH_2PO_4, 1 mmol/L $MgSO_4$, 1 mmol/L $CaCl_2$, and 2 mmol/L sodium pyruvate) supplemented with 200 nM adenosine, 5 mM glucose, and 2% BSA, fat pads were digested with 1.5 mg/mL of type II collagenase (for adipocytes, C6885; Sigma) in KRBH buffer for 45 min with gentle shaking at 37°C. Cell suspension was filtered through a 300-μm nylon filter (Small Parts, Inc.) and then spun at 2,000 rpm for 5 min to separate floating adipocytes from the pellets termed stromal vascular cells (SVCs). Erythrocytes in the SVCs were lysed using the cell lysis buffer (BD Biosciences) prior to collection. Floating primary adipocytes were washed with KRBH buffer and spun twice more to remove the contaminating immune cells. Both SVCs and primary adipocytes were snap frozen for RNA extraction.

Peritoneal macrophages. Mice were injected intraperitoneally with 2 mL 4% thioglycollate (211716; BD Biosciences). Four days later, mice were killed and macrophages were harvested by flushing the peritoneum with cold PBS twice and plated at 2×10^6 cells/mL in Dulbecco's modified Eagle's medium (Cellgro) supplemented with 10% FBS (Sigma) and 1% penicillin/streptomycin (Cellgro). Peritoneal macrophages were treated with 0.1 μg/mL LPS (L4391; Sigma) for 5 h followed by the addition of 0.5 or 5 mmol/L ATP (Sigma) for 30 min followed by protein extraction.

Hematoxylin-eosin histology. Adipose tissues were fixed in 4% formaldehyde, embedded in paraffin, and sectioned by the Cornell Histology Core Facility. Pictures were taken using the Axiovert 200M microscope (Zeiss).

ELISA. Blood was collected in animals upon 4 h fasting during the day. Circulating insulin levels were measured using the kit from Millipore. IL-1β level in circulation and adipose tissue was measured using the ELISA kit from eBioscience per supplier's protocol. For tissue ELISA, a piece of WAT was lysed in 1 mL Tris-based lysis buffer by homogenization and IL-1β level was normalized to total WAT weight.

RNA extraction, Q-PCR, and RT-PCR. RNA extraction from cells and tissues and Q-PCR were carried out as previously described (32) using Trizol plus QIAeasy kit (Qiagen) for adipocytes and adipose tissues with DNase digestion (Roche). Q-PCR data collected on the Roche LightCycler 480 were normalized to ribosomal *l32* gene in the corresponding sample. For RT-PCR, the equivalent amount of RNA was reverse transcribed and amplified by 30 PCR cycles (95°C for 15 s, 55–58°C for 15 s, and 72°C for 20 s). The PCR products were separated on a 1.5% agarose gel and visualized using Bio-Rad ChemiDoc XRS+ system after exposure. Supplementary Table 1 lists primer sequences used in this study.

Western blot and quantitation. Tissues or cells were lysed in Tris-based lysis buffer containing 1% Triton X-100. Total lysates (10–20 μg) were used in a mini–SDS-PAGE as previously described (32). Antibodies specific for *p*-S473 serine/threonine protein kinase AKT (9271S; Cell Signaling), AKT (sc-1618; Santa Cruz), inhibitor of nuclear factor-κB (IκB) (9242; Cell Signaling), caspase-1 p10 (sc-514; Santa Cruz), caspase-3 (9665; Cell Signaling), and arginase-1 (Arg1) (sc-18351; Santa Cruz) were used at 1:1,000–2,000, and for the loading control, heat shock protein 90 (HSP90) (sc-7947; Santa Cruz) was used at 1:6,000. Caspase-1 p20 antibody clone 4B4 (a gift from Dr. Vishva Dixit, Genentech, Inc., San Francisco, CA) was used at 1:400. The secondary antibody goat anti-rabbit IgG horseradish peroxidase (HRP) and goat anti-mouse IgG HRP (1:10,000) were from Bio-Rad, and donkey anti-goat IgG HRP (1:10,000) were from Jackson ImmunoResearch. Quantification of band density was carried out using the ImageLab software of the Bio-Rad ChemiDoc XRS+ system after exposure.

Microarray analysis. Microarray analyses of WAT were performed as previously described (33) with four groups (n = 3–4 mice each): age- and sex-matched WT and *P2X*$_7^{-/-}$ mice under either LFD or 12 weeks of HFD. Genes were filtered according to expression value >20 in greater than two arrays with a minimum of 10 probe sets per gene. This resulted in 16,001 genes that were used to generate the scatter plot. Thereafter, genes were selected that were differentially expressed between HFD and LFD using $q < 0.001$ and fold change >1.5, resulting in 3,097 genes that were used to generate the heat map. Data have been deposited into the GEO datasets (GSE36033).

Statistical analysis. Results are expressed as mean ± SEM. Comparisons between groups were made using either unpaired, two-tailed Student t test of the EXCEL software for two-group comparisons or the two-way ANOVA test with the Bonferroni post-tests of the PRISM software for multigroup comparisons. $P < 0.05$ was considered statistically significant.

RESULTS

Inflammasome activation in WAT coincides with the onset of hyperglycemia and hyperinsulinemia. HFD feeding with 60% calories from fat progressively increased BW, gonadal WAT weight, fasting blood glucose, and insulin levels (Fig. 1*A*). Upon 8 weeks of feeding of 60% HFD, mice developed mild hyperglycemia and hyperinsulinemia. RT-PCR analysis revealed that components of NLRP3 inflammasome such as *Nlrp3*, *Casp1*, *Asc*, *Il1b*, and *Il18* were highly expressed in mouse epididymal adipose tissues, whereas other types of inflammasome sensors such as *Nlrp1*, *Nlrc4*, and *Aim2* were expressed at much lower levels (Fig. 1*B*). Furthermore, most NLRP3 inflammasome components including *Nlrp3*, *Casp1*, *Asc*, and *Il18* were expressed at comparable levels in both adipocytes and SVCs in WAT, whereas *Il1b* was predominantly present in the SVC fraction of WAT (Fig. 1*C*).

Intriguingly, most NLRP3 inflammasome components, including *Nlrp3*, *Asc*, and *Casp1*, were highly responsive to HFD feeding and elevated starting at 6 weeks HFD (Fig. 1*C*), as were other types of inflammasome sensors such as *Nlrp1* and *Nlrc4* (Supplementary Fig. 1). Interestingly, the *Il1b* mRNA level was not changed whereas *Il18* was decreased with HFD (Fig. 1*C*). In support, at the protein levels, procaspase-1 p45 was increased fivefold after 8 weeks HFD (Fig. 1*D* and *E*). The cleaved fragment of caspase-1 p35, a marker for caspase-1 activation (13,16,34,35),

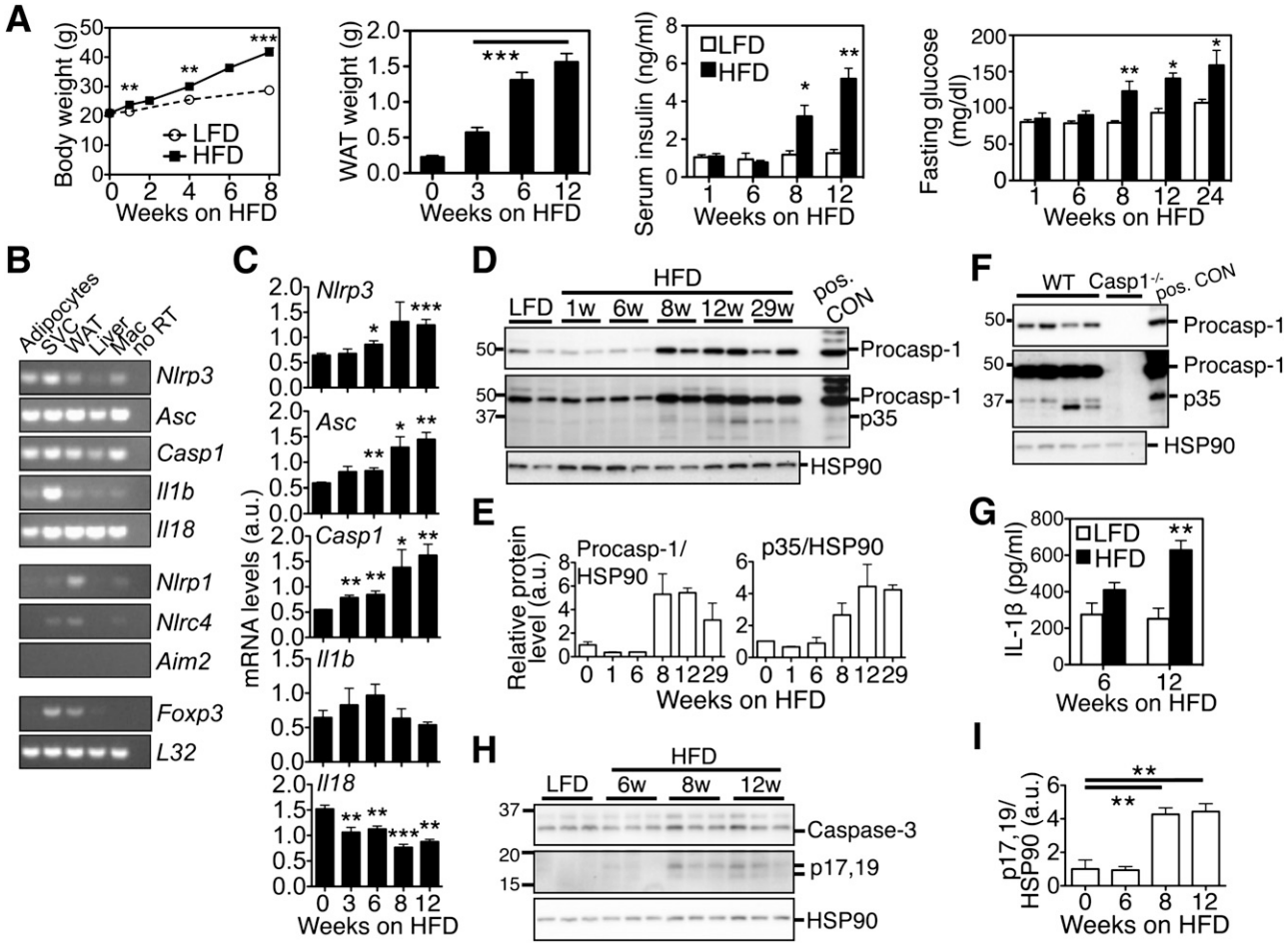

FIG. 1. Inflammasome activation in WAT requires 8 weeks HFD feeding. *A*: Body weight, epididymal WAT weight, insulin levels (following a 4-h fast), and blood glucose (following a 16-h fast) in WT mice on 60% HFD for the indicated time periods from 1 to 24 weeks, compared with age-matched mice on LFD (13% fat); *n* = 6–12 mice each group. *B*: RT-PCR analysis of various inflammasome components in purified primary adipocytes, SVCs, epididymal WAT, liver, and peritoneal macrophages (Mac) of WT mice. The exclusive presence of *Foxp3*, a regulatory T cell–specific marker, in the SVC fraction indicates a clean separation of adipocytes and immune cells in SVCs. *L32*, a loading control; no RT, negative controls with no reverse transcription. *C*: Q-PCR analysis of various inflammasome components in epididymal WAT from HFD-fed WT mice for the indicated time periods, compared with 18-week-old WT mice on LFD (0 weeks on HFD); *n* = 5 mice per group. *D*: Western blot analysis of procaspase-1 p45 (procasp-1) and cleaved caspase-1 p35 in WAT from HFD-fed WT mice with quantification shown in *E*. *F*: Western blot analysis of caspase-1 in WAT from 12- and 29-week HFD–fed WT mice and 16-week HFD–fed *caspase-1*$^{-/-}$ mice, showing the specificity of anti–caspase-1 antibody. Pos. CON, LPS-ATP–treated macrophages. *G*: IL-1β concentration measured in WAT of WT mice on 6 or 12 weeks of 60% HFD, compared with age-matched mice on LFD; *n* = 4–5 mice per group. *H*: Western blot analysis of procaspase-3 and cleaved caspase-3 p17 and p19 in WAT from HFD-fed WT mice with quantification shown in *I*. For Western blots, each lane represents an individual animal or sample with HSP90 as a loading control. All experiments were repeated at least twice. Values represent mean ± SEM. **P* < 0.05, ***P* < 0.01, and ****P* < 0.001, compared to LFD or 0 weeks HFD controls.

exhibited a similar expression pattern (Fig. 1*D* and *E*). The specificity of the caspase-1 antibody was confirmed using adipose tissue from *caspase-1*$^{-/-}$ animals (Fig. 1*F*). Consistently, the IL-1β level in epididymal adipose tissue was significantly increased after 12 weeks, but not 6 weeks, HFD (Fig. 1*G*). Intriguingly, at 8 weeks, not 6 weeks, HFD, cell death in WAT was significantly increased, as measured by levels of cleaved caspase-3 (Fig. 1*H* and *I*), as well as the crown-like structures (Supplementary Fig. 2). Thus, we conclude that inflammasome activation in adipose tissue coincides with increased cell death and the onset of hyperglycemia and hyperinsulinemia.

$P2X_7$ expression in adipose tissue coincides with the activation of inflammasome. Early studies have implicated a significant role of ATP-$P2X_7$ signaling in inflammasome activation in macrophages and dendritic cells and in the clearance of dead cells (18,21,26). However, whether $P2X_7$ plays a role in adipose tissue remains unclear. RT-PCR analyses revealed that among all P2X family members $P2X_{1–7}$, $P2X_7$ was expressed at relatively high levels in both adipocytes and SVCs of mouse epididymal adipose tissue (Fig. 2*A*). Both mRNA and protein levels of $P2X_7$ were significantly increased in the WAT of 13-week-old *ob/ob* mice relative to age-matched WT lean mice (Fig. 2*B* and *C*). Similar observation was obtained in the liver but not muscle or pancreas (Fig. 2*D*).

We next asked when the induction of $P2X_7$ occurred in adipose tissue using HFD-feeding mouse models. Intriguingly, induction of $P2X_7$ protein also occurred at 8 weeks HFD feeding (Fig. 2*E* and *F*), a pattern strikingly similar to that of inflammasome activation. Preceding the induction of its protein, *$P2X_7$* mRNA level was elevated starting at 6 weeks HFD (Fig. 2*G*). Thus, $P2X_7$ protein is induced in adipose tissue after 8 weeks feeding of 60% HFD, coinciding with the activation of inflammasome and the onset of hyperglycemia and hyperinsulinemia.

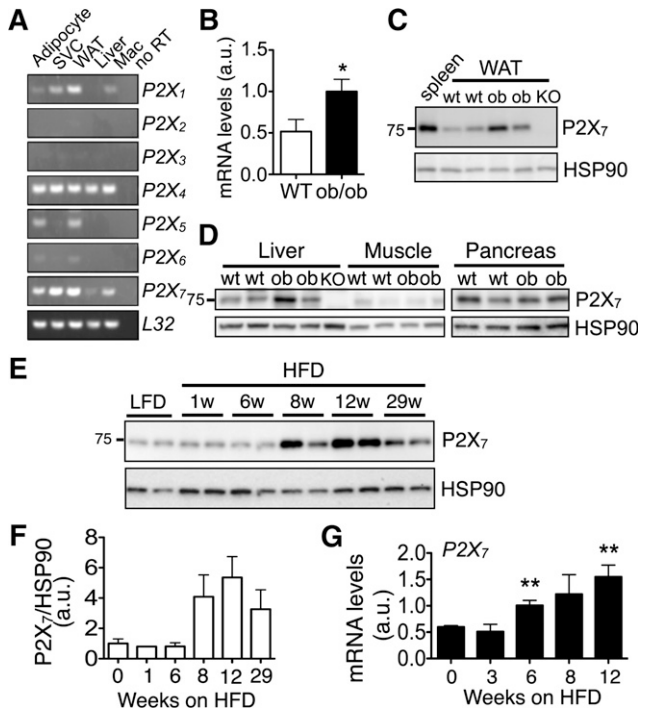

FIG. 2. P2X$_7$ expression is induced in adipose tissue after 8 weeks HFD feeding. *A*: RT-PCR analysis of members of the P2X family in purified primary adipocytes, SVCs, epididymal WAT, liver, and peritoneal macrophages (Mac) of WT mice. *L32*, a loading control; no RT, negative controls with no reverse transcription. *B*: Q-PCR analysis of *P2X$_7$* mRNA levels in the epididymal WAT of 13-week-old *ob/ob* mice in comparison with age- and sex-matched WT mice; n = 5–7 mice per group. *C* and *D*: Western blot analysis of P2X$_7$ in epididymal WAT, liver, muscle, and pancreas from 13-week-old WT and *ob/ob* mice (ob). Spleen from WT mice and WAT/liver from *P2X$_7^{-/-}$* (KO) mice were included as positive and negative controls, respectively. *E*: Western blot analysis of P2X$_7$ in epididymal WAT from HFD-fed WT mice with quantification shown in *F*. *G*: Q-PCR analysis of *P2X$_7$* mRNA levels in epididymal WAT from HFD-fed WT mice, compared with 18-week-old WT mice on LFD (0 weeks on HFD); n = 5 mice per group. HSP90, a loading control. All experiments are representative data from two repeats. Values represent mean ± SEM. **P* < 0.05 and ***P* < 0.01.

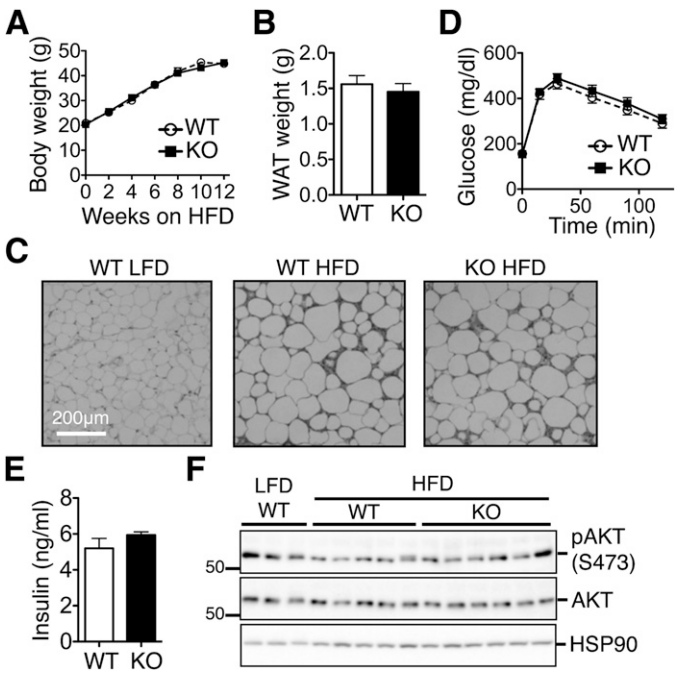

FIG. 3. Whole-body *P2X$_7$* ablation does not affect metabolic status of obese mice. *A*: Body weight of age-matched male WT and *P2X$_7^{-/-}$* (KO) mice upon HFD feeding. *B–F*: Metabolic phenotypes of 18-week-old male mice upon 12 weeks HFD. Epididymal WAT weight (*B*), hematoxylin-eosin staining of WAT sections comparing to WAT from age-matched WT LFD mice (*C*), GTT with 1 g glucose/kg BW after a 16-h fast (*D*), serum insulin level after a 4-h fast (*E*), and Western blot analysis of phosphorylated (*p*-S473) and total AKT after a 4-h fast (*F*). For all, n = 10–29 mice per group. Representative data from two repeats shown. Values represent mean ± SEM.

Whole-body P2X$_7$ ablation does not affect metabolic status in both lean and obese mice. We next addressed whether the ATP-P2X$_7$ signaling axis plays a role in metabolic regulation in HFD-induced obesity by placing *P2X$_7^{-/-}$* mice on 60% HFD feeding for 12 weeks. Obese *P2X$_7^{-/-}$* mice exhibited similar body and gonadal fat weights relative to the WT cohort (Fig. 3*A* and *B*). There were no gross morphological differences in WAT, liver, and pancreas tissues between knockout (KO) and WT cohorts (Fig. 3*C* and Supplementary Fig. 3). Systemic glucose homeostasis and insulin sensitivity were not affected by *P2X$_7$* deficiency as shown by GTT, fasting insulin levels, and AKT phosphorylation, respectively (Fig. 3*D–F*).

Whole-body P2X$_7$ ablation does not affect inflammatory status in obese WAT. Given the known role of P2X$_7$ in ATP-induced inflammasome activation, we next addressed whether the ATP-P2X$_7$ signaling axis is required for inflammasome activation in adipose tissue upon 12 weeks HFD. Unexpectedly, levels of caspase-1 and its cleavage product p35 were not affected in *P2X$_7^{-/-}$* WAT (Fig. 4*A* and *B*), nor was the IL-1β level in WAT (Fig. 4*C*) or mRNA levels of key inflammasome components (Fig. 4*D*), suggesting that P2X$_7$ may be not involved in inflammasome activation in adipose tissue during diet-induced obesity. In direct contrast, *P2X$_7$*-deficient peritoneal macrophages and mice were not able to respond to LPS plus ATP both in vitro (Fig. 4*E*) and in vivo (Fig. 4*F*), further supporting the notion that P2X$_7$ is the only purinergic receptor that activates inflammasome in response to ATP stimulation. Consistently, protein levels of inflammatory markers such as the inhibitor of nuclear factor-κB (IκB) and Arg1 (36,37) in WAT were not affected by *P2X$_7$* deficiency (Fig. 4*A*). In support, the expression of several key pro- and anti-inflammatory genes was not affected by *P2X$_7$* deficiency (Fig. 4*G*). This was further confirmed using an unbiased cDNA microarray analysis of WAT from WT or *P2X$_7^{-/-}$* mice under LFD and 12 weeks HFD where the HFD effect was almost identical between two groups. As shown in both scatter plots and heat map, the loss of *P2X$_7$* had no significant effect on the expression of genes that were regulated by HFD (Fig. 4*H* and Supplementary Fig. 4*A*), including many inflammatory genes (not shown). Taken together, these data suggest that the ATP-P2X$_7$ signaling axis is dispensable for obesity-associated inflammasome activation in WAT.

In addition to P2X$_7$, several other P2 receptors, including P2X$_{1–6}$ and P2Y$_{1–2, 4, 11, 12}$, are capable of sensing extracellular ATP but are not associated with inflammasome activation (38). Loss of *P2X$_7$* did not lead to compensatory increases of other P2 receptors in adipose tissue (Supplementary Fig. 4*B*). Among the P2 family members, *P2Y$_2$*, a G protein–coupled receptor that has been implicated in phagocyte migration in response to extracellular nucleotides released by apoptotic cells (26), is highly expressed in adipose tissue (Supplementary Fig. 4*C*). To further exclude a possible role of P2Y$_2$ in vivo, we characterized the metabolic phenotypes and inflammatory

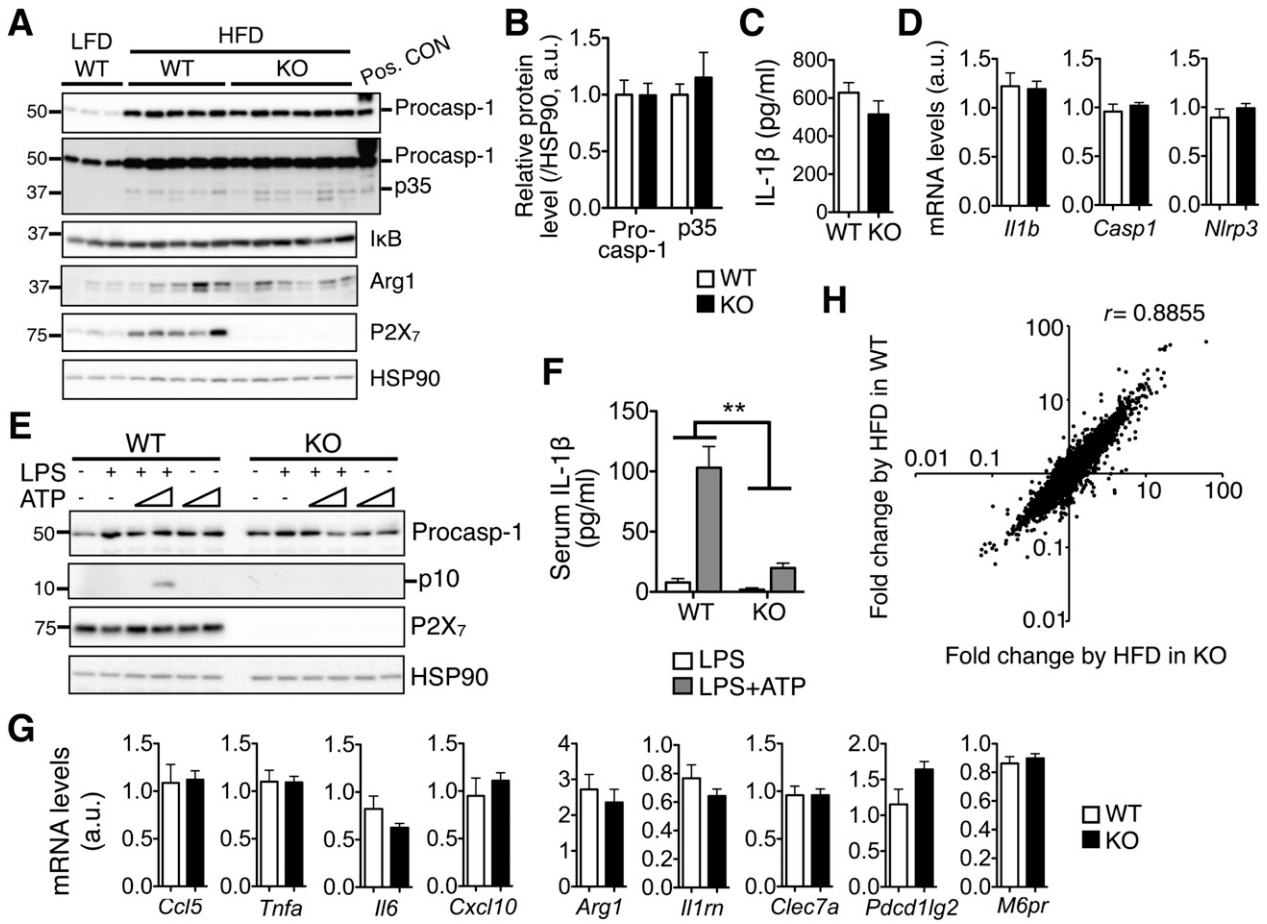

FIG. 4. Whole-body *P2X$_7$* ablation does not affect inflammatory status of obese WAT. *A*: Western blot analysis of caspase-1 p45, p35, IκB, Arg1, and P2X$_7$ protein levels in WAT of age-matched LFD WT, 12-week HFD WT, and *P2X$_7^{-/-}$* (KO) mice. *B*: Quantitation of procaspase 1 and p35. Pos. CON, LPS-ATP–treated macrophages. *C*: IL-1β concentration measured in WAT of 12-week HFD–fed WT and KO mice; *n* = 5 mice per group. *D*: Q-PCR analysis of inflammasome component genes in 12-week HFD–fed WT and KO WAT; *n* = 10 mice per group. *E*: Peritoneal macrophages were treated with LPS (0.1 μg/mL) for 5 h followed by addition of ATP (0.5 or 5 mmol/L) for 30 min, and analyzed for procaspase-1 p45, cleaved caspase-1 p10, and P2X$_7$ protein levels by Western blot analysis. *F*: Serum IL-1β levels in WT and KO mice injected with LPS or LPS plus ATP; *n* = 3 mice per group. *G*: Q-PCR analysis of inflammatory genes in 12-week HFD–fed WT and KO WAT; *n* = 10 mice per group. HSP90, a loading control. All experiments were repeated at least twice. Values represent mean ± SEM. ***P* < 0.01. *H*: Scatter plots of the comparisons of fold changes induced by HFD (vs. LFD) in WAT of WT vs. *P2X$_7^{-/-}$* (KO) mice. Correlation coefficient (*r*) shown; *n* = 3–4 mice each. Heat map shown in Supplementary Fig. 4*A*.

status in WAT of *P2Y$_2^{-/-}$* mice after 15 weeks HFD (Supplementary Fig. 5). We failed to observe any alternations in metabolic phenotypes (Supplementary Fig. 5*A*–*E*), inflammatory responses (Supplementary Fig. 5*F* and *G*), or inflammasome activation (Supplementary Fig. 5*G* and *H*) in adipose tissue compared with age-matched WT controls. These results excluded the involvement of another ATP receptor, P2Y$_2$, in inflammasome activation in obese WAT.

P2X$_7$ ablation in hematopoietic cells does not affect inflammatory status in obese WAT. To exclude a possible role of P2X$_7$ in somatic cells, such as pancreatic β-cells (39) and adipocytes (40), that may affect the outcome of inflammasome activation in adipose tissue, we next specifically ablated *P2X$_7$* in hematopoietic cells using BMT. Preliminary BMT experiments using congenic CD45.1$^+$ and CD45.2$^+$ mice showed efficient immune cell reconstitution in SVCs of WAT (Supplementary Fig. 6). Next, lethally irradiated WT mice were reconstituted with bone marrow from *P2X$_7^{-/-}$* or WT mice. Metabolic phenotypes and inflammasome status were examined after 16 weeks HFD after 4 weeks recovery (Fig. 5*A*). The loss of *P2X$_7$* in hematopoietic cells did not affect BW gain, fat weight, and adipose tissue morphology (Fig. 5*B*–*D*). Liver and pancreas tissue morphologies were also comparable between experimental and control cohorts (Supplementary Fig. 7). Systemic glucose tolerance and fasting insulin levels were not affected by hematopoietic-specific *P2X$_7$* ablation (Fig. 5*E* and *F*). Moreover, mice with *P2X$_7$* deficiency in hematopoietic cells exhibited no alterations in inflammasome activity as shown by the protein levels of caspase-1 p45 and p35 (Fig. 6*A* and *B*) as well as mRNA levels of three key inflammasome components (Fig. 6*C*). Additionally, the overall inflammation level in WAT was not altered, as shown by protein levels of IκB (Fig. 6*A*) and mRNA levels of various inflammatory genes (Fig. 6*D*). Thus, these data suggest that hematopoietic P2X$_7$ is not required for inflammasome activation in obese adipose tissue.

DISCUSSION

Previous studies have shown that inflammasome is activated in obese adipose tissue either after 36 weeks 60% HFD or 12 weeks 45% HFD feeding (13,15), and it remains unclear how long it takes for HFD feeding to activate inflammasome in adipose tissue. Here, we report a dramatic activation of inflammasome in adipose tissue starting at 8 weeks feeding

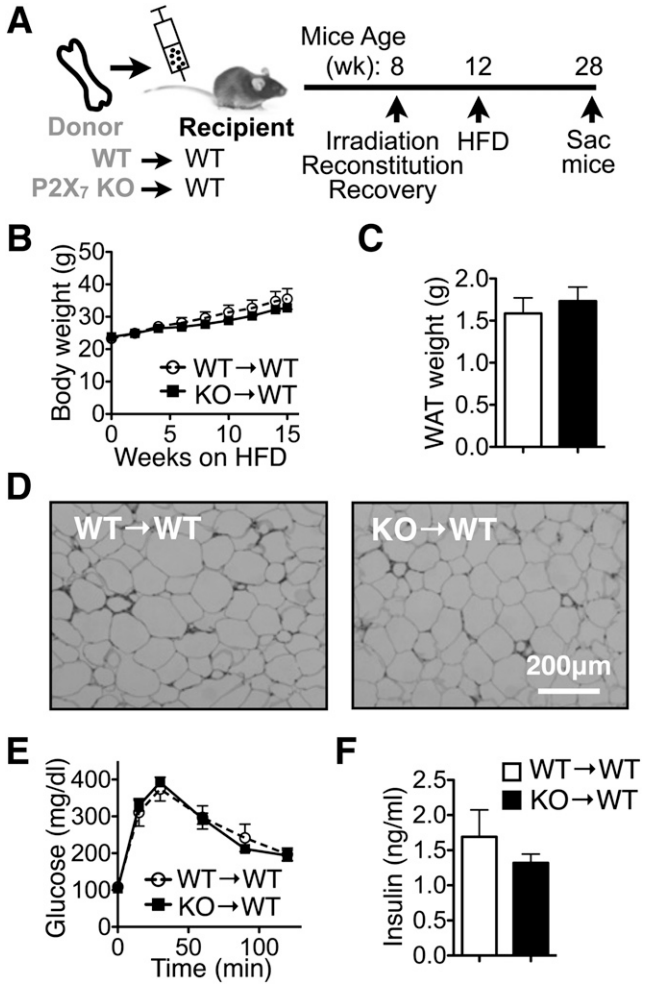

FIG. 5. *P2X$_7$* ablation in hematopoietic cells does not affect metabolic status of obese mice. *A*: Schematic diagram of generation of BMT chimeric mice followed by 4 weeks recovery and 16 weeks HFD feeding. *B*: Body weight of age-matched chimeric mice upon HFD feeding. *C–F*: Metabolic phenotypes of 28-week-old chimeric mice upon 16 weeks HFD. Epididymal WAT weight (*C*), hematoxylin-eosin staining of WAT sections (*D*), GTT with 1 g glucose/kg BW after a 16-h fast (*E*), and serum insulin level after a 4-h fast (*F*). For all, n = 7–8 mice per group. All experiments repeated twice. Values represent mean ± SEM.

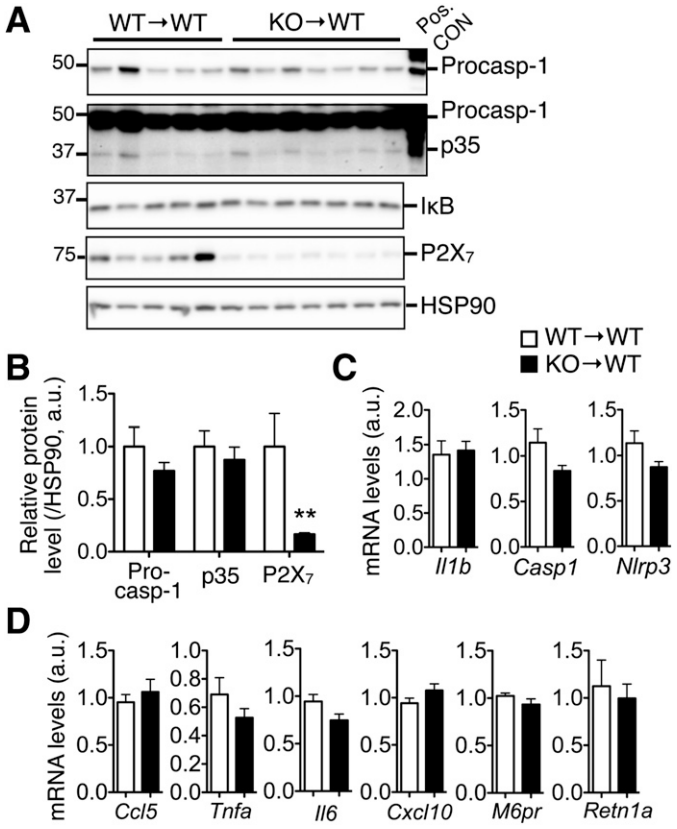

FIG. 6. *P2X$_7$* ablation in hematopoietic cells does not affect inflammasome activation of obese WAT. Western blot analysis (*A*) and quantification (*B*) of caspase-1 p45, p35, IκB, and P2X$_7$ protein levels in epididymal WAT from chimeric mice; n = 5–7 mice per group. Pos. CON, LPS-ATP–treated macrophages. HSP90, a loading control. Q-PCR analysis of inflammasome (*C*) and inflammatory genes (*D*) in epididymal WAT from chimeric mice; n = 7–8 mice per group. All experiments were repeated twice. Values represent mean ± SEM. **$P < 0.01$.

of 60% HFD, coinciding with the onset of hyperglycemia and hyperinsulinemia and with cell death. This is consistent with the general timeline of inflammation during diet-induced obesity, which was reported to be up-regulated at 9 weeks in adipose tissue based on the infiltration of macrophages with 60% HFD and the global induction of inflammatory genes in microarray analysis with 45% HFD (28,41). In parallel with the onset of inflammation, cell death in adipose tissue was elevated at about 4–8 weeks 60% HFD and peaked at about 12 weeks HFD (Fig. 1*H* and *I* and Supplementary Fig. 2) (28). These tight correlations among HFD feeding, cell death, and inflammatory response strongly suggest that dying cells in obese adipose tissue may release cell death–mediated "danger signals" to activate inflammasome in situ. However, our data demonstrate that extracellular ATP-P2X$_7$ signaling is not involved in inflammasome activation in obese adipose tissue in vivo. This observation is in line with a recent study showing that adipocyte cell death is not sufficient to drive inflammation (30).

We observed that P2X$_7$, an inflammasome-activating ATP receptor in several disease models (17–21,23,26), was highly induced at 8 weeks HFD, coinciding with the inflammasome activation in obese adipose tissue. In line with our observation, a recent study showed that *P2X$_7$* expression is increased in adipose tissue of human patients with metabolic syndrome (42). However, our data demonstrated that, although required for LPS-ATP–induced inflammasome activation both in vitro and in vivo (Fig. 4*E* and *F*), P2X$_7$ is dispensable for inflammasome activation in obese adipose tissue in vivo. One possible explanation is that the extent of cell death in adipose tissue during obesity may be much lower than the systems used in previous studies, such as drug-induced tumor cell death, host-verses-graft disease, and sterile inflammasome (12–15). Additionally, ATP may be quickly hydrolyzed in extracellular space (22,43). Therefore, as P2X$_7$ receptor requires a high ATP level to be activated (~5 mM) (Fig. 4*E*) (43), extracellular ATP in obese adipose tissue may not reach the activation threshold for P2X$_7$ and thus fail to activate inflammasome in vivo. This possibility is supported by a study showing that *CD39*$^{-/-}$ mice, which are incapable of hydrolyzing extracellular ATP, exhibit exacerbated insulin resistance (44). Although the inflammatory status was not examined in the *CD39*$^{-/-}$ mice, this report suggests that extracellular ATP may have a metabolic effect when it reaches a certain level.

Though our data suggest that extracellular ATP may not be the "danger signal" for inflammasome activation in WAT

during obesity, it does not exclude the potential importance of cell stress and death in obese adipose tissue during the pathogenesis of obesity. Lipid spillover during adipocyte expansion and death has been linked to macrophage infiltration and obesity-associated inflammation (45). Indeed, several studies using lipodystrophy mouse models suggest that adipocyte cell death is important for macrophage infiltration into adipose tissue (46,47). Furthermore, both palmitate and ceramides, but not unsaturated oleate, have been reported to activate NLRP3 inflammasome in bone marrow–derived macrophages in vitro (14,15). As saturated fatty acid has been demonstrated to induce ceramide biosynthesis in vivo (48), it remains to be tested whether palmitate and ceramides activate inflammasome in adipose tissue via the same mechanism. Thus, the function of lipids as inflammasome-activating signals in obese adipose tissue and the underlying molecular mechanism are worth further studies.

Alternatively, inflammasome in obese adipose tissue may be activated by mechanisms unrelated to in situ cell death. A high glucose level has been suggested to induce inflammasome activation. In isolated pancreatic islets, a high glucose level was shown to induce thioredoxin interacting protein (TXNIP) expression and then activate inflammasome, which was not mediated by ATP-$P2X_7$ signaling (12). In another independent study, similar induction of TXNIP and IL-1β by glucose was observed in adipose tissue explants and primary adipocytes (16). These reports indicate that hyperglycemia during obesity may lead to inflammasome activation. Interestingly, we observed that the onset of both hyperglycemia and inflammasome activation in adipose tissue occurred at 8 weeks HFD, whereas 6 weeks HFD feeding was not sufficient. Further studies are needed to show the potential role of high circulating glucose levels in inflammasome activation in adipose tissue in vivo.

To date, four classes of inflammasomes have been shown to activate caspase-1 in vivo, including NLRP3, NLRP1, NLRC4, and AIM2 inflammasome (10). Different classes of inflammasomes may respond to specific environmental cues. For example, the NLRC4 inflammasome is activated by gram-negative bacteria, the AIM2 inflammasome senses cytosolic double-stranded DNA, and the NLRP3 inflammasome responds to a number of pathogen-associated or endogenous danger–associated activators (10). Previous studies on inflammasomes in adipose tissue focused on NLRP3 inflammasome (13,15). However, the nature of inflammasomes in adipose tissue remains unclear and their cell-type specificity has not been examined. Here, we determined the expression of the four classes of inflammasomes in epididymal adipose tissue and liver by assessing the relative transcript levels of their sensors. Besides NLRP3, our data show that both NLRP1 and NLRC4 were also expressed in adipose tissue and were highly induced after 8 weeks HFD. In contrast, AIM2 expression was very low in adipose tissue. Thus, the role of non-NLRP3 inflammasomes in adipose inflammation in obesity requires further investigation.

Inflammasome activation generates two active caspase-1 subunits, p20 and p10, with enzymatic activities (10). In addition, as first reported by Tschopp and colleagues (34) in a cell-free system, the caspase-1 intermediate product p35 may also serve as an indicator for the activation of caspase-1. Recently, several studies by different groups have used p35 as a marker of inflammasome activation in tissues (13,16,35). Indeed, our data show that the p35 band is caspase-1 specific as it disappears in the caspase-1–deficient adipose tissue (Fig. 1*F*), and more importantly, that the appearance of caspase-1 p35 subunit in WAT under various physiological settings is in line with that of caspase-1 p20 (Fig. 1*D* and *F*, Fig. 4*A*, and Fig. 6*A* vs. Supplementary Fig. 8). Thus, the caspase-1 p35 fragment, albeit possibly not the active form, may be a bona fide indicator of inflammasome status in WAT.

$P2X_7$ was previously reported to regulate pancreatic β-cell functions by modulating insulin secretion and β-cell mass (39). Upon feeding with high-fat/high-sucrose Surwit diet (58% fat with majority of saturated fat, 26% carbohydrate, and 16% protein, no fiber) for 12 weeks, $P2X_7^{-/-}$ mice developed hyperglycemia, severe glucose intolerance, decreased β-cell mass, and impaired β-cell function (39). Such β-cell–associated diabetic phenotype, however, was not observed in our study (Fig. 3 and Supplementary Figs. 3 and 7). The discrepancies may be due to specific diets used in the studies. In addition, the ATP-$P2X_7$ signaling axis has been reported to induce lipolysis and inhibit insulin signaling in adipocytes in vitro by upregulating cyclic AMP levels or inhibiting phosphorylation on insulin receptor substrate and AKT in rat primary adipocytes (40,49,50). In contrast, others have reported that insulin signaling was downregulated by ATP-$P2X_7$ in astrocytes (51,52). Here in our study, animals with both global and hematopoietic-specific deletion of $P2X_7$ did not exhibit altered systemic insulin sensitivity and adiposity, suggesting a dispensable role of ATP-$P2X_7$ signaling in regulating adipocyte function and insulin sensitivity in vivo.

In conclusion, our study showed that inflammasome is activated concurrently with the development of hyperglycemia and hyperinsulinemia. Unexpectedly, the ATP-$P2X_7$ signaling axis seems not to play a critical role in this process. Further studies are required to identify and characterize the endogenous signal(s) that is responsible for inflammasome activation in adipose tissue during obesity.

ACKNOWLEDGMENTS

S.S. is supported by the International Student Research Fellowship from the Howard Hughes Medical Institute. This study was also funded by the Netherlands Nutrigenomics Centre (to S.K.), Cornell startup package, American Diabetes Association (7-08-JF-47 and 1-12-CD-04), and National Institute of Diabetes and Digestive and Kidney Diseases (R01-DK-082582 and R01-DK-082582-S1 to L.Q.).

No potential conflicts of interest relevant to this article were reported.

S.S. conceived the framework of the study, designed the experiments, performed most in vivo and in vitro studies, analyzed data, and wrote, commented on, and approved the manuscript. S.X. performed the flow cytometric analysis of BMT, analyzed data, and commented on and approved the manuscript. Y.J. helped with animal dissections and Q-PCR analysis, analyzed data, and commented on and approved the manuscript. S.K. performed the microarray analysis, analyzed data, and commented on and approved the manuscript. L.Q. conceived the framework of the study, designed the experiments, analyzed data, and edited, commented on, and approved the manuscript. L.Q. is the guarantor of this work and, as such, had full access to all the data in the study and takes responsibility for the integrity of the data and the accuracy of the data analysis.

Parts of this study have been submitted in abstract form for presentation at the 72nd Scientific Sessions of the American Diabetes Association, Philadelphia, Pennsylvania, 8–12 June 2012.

The authors thank Dr. Rinke Stienstra for helpful suggestions and sharing *Casp1*$^{-/-}$ WAT, Dr. Joseph Wakshlag (Cornell University) and Dr. Vishva Dixit for caspase-3 and caspase-1 p20 antibodies, Dr. Qiaoming Long (Cornell University) for use of the microscope, Cindy Wang (Cornell University) for technical assistance, and other members of the Qi Laboratory at Cornell University for critical discussions/suggestions.

REFERENCES

1. Hotamisligil GS, Shargill NS, Spiegelman BM. Adipose expression of tumor necrosis factor-alpha: direct role in obesity-linked insulin resistance. Science 1993;259:87–91
2. Hotamisligil GS, Arner P, Caro JF, Atkinson RL, Spiegelman BM. Increased adipose tissue expression of tumor necrosis factor-alpha in human obesity and insulin resistance. J Clin Invest 1995;95:2409–2415
3. Xu H, Barnes GT, Yang Q, et al. Chronic inflammation in fat plays a crucial role in the development of obesity-related insulin resistance. J Clin Invest 2003;112:1821–1830
4. Weisberg SP, McCann D, Desai M, Rosenbaum M, Leibel RL, Ferrante AW Jr. Obesity is associated with macrophage accumulation in adipose tissue. J Clin Invest 2003;112:1796–1808
5. Olefsky JM, Glass CK. Macrophages, inflammation, and insulin resistance. Annu Rev Physiol 2010;72:219–246
6. Jager J, Grémeaux T, Cormont M, Le Marchand-Brustel Y, Tanti JF. Interleukin-1beta-induced insulin resistance in adipocytes through down-regulation of insulin receptor substrate-1 expression. Endocrinology 2007;148:241–251
7. Lagathu C, Yvan-Charvet L, Bastard J-P, et al. Long-term treatment with interleukin-1beta induces insulin resistance in murine and human adipocytes. Diabetologia 2006;49:2162–2173
8. Larsen CM, Faulenbach M, Vaag A, et al. Interleukin-1-receptor antagonist in type 2 diabetes mellitus. N Engl J Med 2007;356:1517–1526
9. Netea MG, Joosten LAB, Lewis E, et al. Deficiency of interleukin-18 in mice leads to hyperphagia, obesity and insulin resistance. Nat Med 2006;12:650–656
10. Schroder K, Tschopp J. The inflammasomes. Cell 2010;140:821–832
11. Pétrilli V, Dostert C, Muruve DA, Tschopp J. The inflammasome: a danger sensing complex triggering innate immunity. Curr Opin Immunol 2007;19:615–622
12. Zhou R, Tardivel A, Thorens B, Choi I, Tschopp J. Thioredoxin-interacting protein links oxidative stress to inflammasome activation. Nat Immunol 2010;11:136–140
13. Stienstra R, Joosten LAB, Koenen T, et al. The inflammasome-mediated caspase-1 activation controls adipocyte differentiation and insulin sensitivity. Cell Metab 2010;12:593–605
14. Wen H, Gris D, Lei Y, et al. Fatty acid-induced NLRP3-ASC inflammasome activation interferes with insulin signaling. Nat Immunol 2011;12:408–415
15. Vandanmagsar B, Youm Y-H, Ravussin A, et al. The NLRP3 inflammasome instigates obesity-induced inflammation and insulin resistance. Nat Med 2011;17:179–188
16. Koenen TB, Stienstra R, van Tits LJ, et al. Hyperglycemia activates caspase-1 and TXNIP-mediated IL-1beta transcription in human adipose tissue. Diabetes 2011;60:517–524
17. Di Virgilio F. Liaisons dangereuses: P2X(7) and the inflammasome. Trends Pharmacol Sci 2007;28:465–472
18. McDonald B, Pittman K, Menezes GB, et al. Intravascular danger signals guide neutrophils to sites of sterile inflammation. Science 2010;330:362–366
19. Weber FC, Esser PR, Müller T, et al. Lack of the purinergic receptor P2X(7) results in resistance to contact hypersensitivity. J Exp Med 2010;207:2609–2619
20. Ghiringhelli F, Apetoh L, Tesniere A, et al. Activation of the NLRP3 inflammasome in dendritic cells induces IL-1beta-dependent adaptive immunity against tumors. Nat Med 2009;15:1170–1178
21. Wilhelm K, Ganesan J, Müller T, et al. Graft-versus-host disease is enhanced by extracellular ATP activating P2X7R. Nat Med 2010;16:1434–1438
22. Corriden R, Insel PA. Basal release of ATP: an autocrine-paracrine mechanism for cell regulation. Sci Signal 2010;3:re1
23. Khakh BS, North RA. P2X receptors as cell-surface ATP sensors in health and disease. Nature 2006;442:527–532
24. Mariathasan S, Weiss DS, Newton K, et al. Cryopyrin activates the inflammasome in response to toxins and ATP. Nature 2006;440:228–232
25. Tschopp J, Schroder K. NLRP3 inflammasome activation: the convergence of multiple signalling pathways on ROS production? Nat Rev Immunol 2010;10:210–215
26. Elliott MR, Chekeni FB, Trampont PC, et al. Nucleotides released by apoptotic cells act as a find-me signal to promote phagocytic clearance. Nature 2009;461:282–286
27. Cinti S, Mitchell G, Barbatelli G, et al. Adipocyte death defines macrophage localization and function in adipose tissue of obese mice and humans. J Lipid Res 2005;46:2347–2355
28. Strissel KJ, Stancheva Z, Miyoshi H, et al. Adipocyte death, adipose tissue remodeling, and obesity complications. Diabetes 2007;56:2910–2918
29. Alkhouri N, Gornicka A, Berk MP, et al. Adipocyte apoptosis, a link between obesity, insulin resistance, and hepatic steatosis. J Biol Chem 2010;285:3428–3438
30. Feng D, Tang Y, Kwon H, et al. High-fat diet-induced adipocyte cell death occurs through a cyclophilin D intrinsic signaling pathway independent of adipose tissue inflammation. Diabetes 2011;60:2134–2143
31. Pajvani UB, Trujillo ME, Combs TP, et al. Fat apoptosis through targeted activation of caspase 8: a new mouse model of inducible and reversible lipoatrophy. Nat Med 2005;11:797–803
32. Sha H, He Y, Chen H, et al. The IRE1alpha-XBP1 pathway of the unfolded protein response is required for adipogenesis. Cell Metab 2009;9:556–564
33. Lichtenstein L, Mattijssen F, de Wit NJ, et al. Angptl4 protects against severe proinflammatory effects of saturated fat by inhibiting fatty acid uptake into mesenteric lymph node macrophages. Cell Metab 2010;12:580–592
34. Martinon F, Burns K, Tschopp J. The inflammasome: a molecular platform triggering activation of inflammatory caspases and processing of proIL-beta. Mol Cell 2002;10:417–426
35. Martinon F, Pétrilli V, Mayor A, Tardivel A, Tschopp J. Gout-associated uric acid crystals activate the NALP3 inflammasome. Nature 2006;440:237–241
36. Bellenger J, Bellenger S, Bataille A, et al. High pancreatic n-3 fatty acids prevent STZ-induced diabetes in fat-1 mice: inflammatory pathway inhibition. Diabetes 2011;60:1090–1099
37. Ishii M, Wen H, Corsa CAS, et al. Epigenetic regulation of the alternatively activated macrophage phenotype. Blood 2009;114:3244–3254
38. Skaper SD, Debetto P, Giusti P. The P2X7 purinergic receptor: from physiology to neurological disorders. FASEB J 2010;24:337–345
39. Glas R, Sauter NS, Schulthess FT, Shu L, Oberholzer J, Maedler K. Purinergic P2X7 receptors regulate secretion of interleukin-1 receptor antagonist and beta cell function and survival. Diabetologia 2009;52:1579–1588
40. Lee H, Jun DJ, Suh BC, et al. Dual roles of P2 purinergic receptors in insulin-stimulated leptin production and lipolysis in differentiated rat white adipocytes. J Biol Chem 2005;280:28556–28563
41. Kleemann R, van Erk M, Verschuren L, et al. Time-resolved and tissue-specific systems analysis of the pathogenesis of insulin resistance. PLoS ONE 2010;5:e8817
42. Madec S, Rossi C, Chiarugi M, et al. Adipocyte P2X7 receptors expression: a role in modulating inflammatory response in subjects with metabolic syndrome? Atherosclerosis 2011;219:552–558
43. North RA. Molecular physiology of P2X receptors. Physiol Rev 2002;82:1013–1067
44. Enjyoji K, Kotani K, Thukral C, et al. Deletion of cd39/entpd1 results in hepatic insulin resistance. Diabetes 2008;57:2311–2320
45. Kosteli A, Sugaru E, Haemmerle G, et al. Weight loss and lipolysis promote a dynamic immune response in murine adipose tissue. J Clin Invest 2010;120:3466–3479
46. Fischer-Posovszky P, Wang QA, Asterholm IW, Rutkowski JM, Scherer PE. Targeted deletion of adipocytes by apoptosis leads to adipose tissue recruitment of alternatively activated M2 macrophages. Endocrinology 2011;152:3074–3081
47. Herrero L, Shapiro H, Nayer A, Lee J, Shoelson SE. Inflammation and adipose tissue macrophages in lipodystrophic mice. Proc Natl Acad Sci USA 2010;107:240–245
48. Holland WL, Bikman BT, Wang L-P, et al. Lipid-induced insulin resistance mediated by the proinflammatory receptor TLR4 requires saturated fatty acid-induced ceramide biosynthesis in mice. J Clin Invest 2011;121:1858–1870
49. Hashimoto N, Robinson FW, Shibata Y, Flanagan JE, Kono T. Diversity in the effects of extracellular ATP and adenosine on the cellular processing and physiologic actions of insulin in rat adipocytes. J Biol Chem 1987;262:15026–15032
50. Yu Z, Jin T. Extracellular high dosages of adenosine triphosphate induce inflammatory response and insulin resistance in rat adipocytes. Biochem Biophys Res Commun 2010;402:455–460
51. Liu Y-P, Yang C-S, Chen M-C, Sun SH, Tzeng SF. Ca(2+)-dependent reduction of glutamate aspartate transporter GLAST expression in astrocytes by P2X(7) receptor-mediated phosphoinositide 3-kinase signaling. J Neurochem 2010;113:213–227
52. Neary JT, Kang Y. P2 purinergic receptors signal to glycogen synthase kinase-3beta in astrocytes. J Neurosci Res 2006;84:515–524